HHS Public Access

Author manuscript

Nat Struct Mol Biol. Author manuscript; available in PMC 2018 May 14.

Published in final edited form as:

Nat Struct Mol Biol. 2016 September ; 23(9): 865–867. doi:10.1038/nsmb.3268.

Extended Surface for Membrane Association in Zika Virus NS1 Structure

W. Clay Brown[1,†], **David L. Akey**[1,†], **Jamie Konwerski**[1], **Jeffrey T. Tarrasch**[1], **Georgios Skiniotis**[1,2], **Richard J. Kuhn**[3], and **Janet L. Smith**[1,2,*]

[1]Life Sciences Institute, University of Michigan, Ann Arbor, Michigan, USA

[2]Department of Biological Chemistry, University of Michigan, Ann Arbor, Michigan, USA

[3]Purdue Institute for Inflammation, Immunology and Infectious Disease, Purdue University, West Lafayette, Indiana, USA

Abstract

The Zika virus, which is implicated in an increase in neonatal microcephaly and Guillain-Barré syndrome, has spread rapidly through tropical regions of the world. The virulence protein NS1 functions in genome replication and host immune system modulation. Here we report the crystal structure of full-length Zika virus NS1, revealing an elongated hydrophobic surface for membrane association and a polar surface that varies substantially among flaviviruses.

Zika virus (ZIKV) is the cause of a current international public health emergency due to its rapid spread in the Americas[1] and anticipated increase in habitats of the *Aedes aegypti* mosquito vector. Although ZIKV has been in circulation in tropical regions of the world for more than 60 years[2], a causative association with severe congenital microcephaly via placental transmission[3,4] and an association with Guillain-Barré syndrome in adults[5] were not identified until the 2015 outbreak in Brazil. The lack of effective vaccines, antiviral treatments and rapid detection methods places urgency on detailed investigations of ZIKV and distinct aspects of its life cycle.

ZIKV is a flavivirus, related to dengue (DENV), West Nile (WNV) and Japanese encephalitis viruses (JEV)[6,7]. The flavivirus positive-sense RNA genome encodes three structural proteins, which form the virus particle, and seven nonstructural proteins, which perform essential functions in genome replication, polyprotein processing, and manipulation

*Correspondence to: JanetSmith@umich.edu.
†These authors contributed equally to this work.

Accession code

The atomic coordinates and structure factors for the ZIKV NS1 structure are deposited in the Protein Data Bank with accession code 5K6K.

Author Contributions

W.C.B., D.L.A., R.J.K. and J.L.S. planned the experiments; W.C.B. created expression constructs; J.K. purified and crystallized the protein; D.L.A. solved the crystal structure; J.T.T. and G.S. carried out the electron microscopy analysis; W.C.B., D.L.A., R.J.K. and J.L.S. wrote the paper.

Competing Financial Interests Statement

The authors state no competing financial interests.

of cellular processes to viral advantage. Flavivirus nonstructural protein 1 (NS1), one of only ten viral proteins, is a multi-functional virulence factor[8,9]. Within an infected cell, the glycosylated 48-kDa NS1 is a membrane-associated dimer following translocation into the endoplasmic reticulum (ER) lumen, where it is essential for viral genome replication. The replication complex at the ER membrane includes NS1 on the lumen side, viral transmembrane proteins (NS2a, NS2b, NS4a, NS4b), and viral enzymes (NS3 protease-helicase, NS5 capping enzyme and RNA-dependent RNA polymerase) on the cytoplasmic side. Infected cells also secrete NS1 as a hexameric lipo-protein particle[10], which is detected in the serum of infected individuals at levels correlated with disease severity. NS1 also associates with the surface of infected cells where its role is unclear. Crystal structures from our lab established details of the dimer and hexamer architecture of NS1 from dengue virus serotype 2 (DENV2) and WNV[11]. Secreted NS1 (sNS1) interacts with complement system proteins and has several immune-modulatory functions. In an animal model, DENV NS1, in the absence of virus, can lead to vascular leakage typical of severe dengue infection[12], possibly by activating macrophages via the Toll-like receptor 4[13]. sNS1 is a component of some dengue virus candidate vaccines. Structure-based mutagenesis implied additional unexpected NS1 functions during virus maturation, including interaction with the viral prM and envelope proteins[14].

As molecular studies are lacking, we infer the overall characteristics of the ZIKV infection cycle from results on several flaviviruses, especially the DENV, WNV and JEV. Recent electron cryo-microscopy characterization of the structures of the mature virus particle[15,16] and a crystal structure of the C-terminal half of NS1[17] provided details specific to ZIKV. We sought complete structural details to understand ZIKV NS1 function and solved a 1.9-Å structure of the full-length protein from the original Uganda strain, providing insights to membrane interaction and variability in the protein surfaces.

Flavivirus NS1 encompasses three distinct domains, an N-terminal β-roll, an epitope-rich wing domain, and a C-terminal β-ladder[11,18]. Twelve invariant cysteines form six disulfide bonds per monomer. The fundamental unit is a flat, cross-shaped dimer, formed via the intertwined β-roll and end-to-end β-ladders (Fig. 1). On the “inner” face of the dimer, the β-roll domain and an adjacent “greasy finger” loop form a hydrophobic surface that is the prime candidate for membrane interaction, as it is adjacent to amino acids implicated in contacts with the viral transmembrane proteins[19]. The dimer “outer” face is polar and contains the glycosylation sites. In the NS1 hexamer, three dimers assemble with the glycosylated, polar faces pointed outward and the hydrophobic faces pointed inward where they can interact with lipid molecules in the sNS1 lipo-protein particle.

In its protein fold and domain arrangement, ZIKV NS1 (Fig. 1a,b; Supplementary Table 1) is virtually identical to DENV2 and WNV NS1[11]. The wing domain positions differ by less than 3° rotation relative to the central β-ladder. Despite this overall similarity, the ZIKV NS1 crystal structure provides important new information about a wing domain flexible loop (residues 108-129) that was not visibile in previous structures.

The hydrophobic surface identified in WNV NS1, including the β-roll and a “greasy finger”, [11] is expanded in ZIKV NS1 due to the stabilization of two regions that were disordered

(wing flexible loop) or poorly ordered (27–30) in the previous structures (Fig. 2). Interestingly, these segments lie on the inner hydrophobic face of NS1 and include three highly conserved Trp residues as well as the dipeptide 123-124, which is hydrophobic in all NS1 sequences and in more than 90% contains an aromatic residue (Supplementary Fig. 1). The aromatic side chains in the flexible loop provide a striking outward expansion of the hydrophobic surface to include the ends of the wing domains (Fig. 2b,c). Together with Trp28 in the β-roll domain and Phe163 in the greasy finger, Trp115, Trp118 and Phe123 protrude from the dimer inner hydrophobic face and form an array of conserved aromatic groups that supply additional anchor points for membrane association, particularly with the interfacial region of the membrane bilayer (Fig. 2c,d).

The aromatic amino acids on the ZIKV NS1 wing flexible loop appear in a membrane-interacting position, but evidence suggests that this is not the only loop conformation. Linear epitopes mapped to NS1 occur with high frequency in the flexible loop (www.iedb.org), and a high degree of flexibility is indicated by the lack of electron density for the loop in previous crystal structures, which include a total of 10 views of the WNV and DENV2 NS1 polypeptides. None of the flexible loop aromatic side chains pack into the interior of the wing domain in any crystal structure, and we therefore conclude that they are involved in interactions with the membrane, with lipids, and perhaps also with other proteins, consistent with recent mutational studies that showed an interaction of DENV NS1 Trp115 with the envelope proteins, presumably in the context of virions[14].

Another aspect of NS1 is its secreted lipo-protein hexameric form. Crystal structures of lipid-free WNV and DENV2 NS1 proteins revealed a hexameric association of three dimers with the hydrophobic surfaces pointed inward[11], as expected for a lipid complex. We purified lipid-free, recombinant ZIKV NS1, and observed two distinct species: one consistent in size with an NS1 hexamer and the other with a dimer, which yielded the crystal structure reported here. To examine whether ZIKV NS1 forms a hexamer similar to previously studied flavivirus NS1 proteins, we visualized the hexamer fraction by negative stain electron microscopy (Fig. 3a, Supplementary Fig. 2). Two-dimensional class averages of ZIKV NS1 show hexameric particles, consistent in both size and shape with hexamers of WNV and DENV2 NS1[10,11,20]. The superposition of the ZIKV NS1 dimer on the DENV2 NS1 hexamer structure provides a model for the lipoprotein hexamer of ZIKV NS1 (Fig. 3b,c). In this model, the wing flexible loop is directed inward, towards the lipid cargo. The ordered loop spans a gap between dimers, and could potentially stabilize the hexamer. As the loop residues were not visible in previous crystal structures, it is likely that these segments have different conformations in the context of lipid or protein association of sNS1.

Of the two faces of NS1, the outer polar face exhibits the greater degree of sequence diversity[11]. This has implications for immune system recognition and vaccine development as the outer face is more likely to elicit an immune response, whether on the cell surface or as a secreted lipoprotein. Even within only the central β-ladder domain, ZIKV NS1 has differences in the electrostatic surface potential compared to DENV and WNV NS1[17]. With the structure of full-length ZIKV NS1, we can now visualize the surface differences in the context of the complete NS1 proteins, and therefore modeled NS1 from an isolate in the Brazil outbreak. $ZIKV_{Brazil}$ NS1 and $ZIKV_{Uganda}$ NS1 differ by two non-conservative

changes: $Glu146_{Uganda}$ *vs.* $Lys146_{Brazil}$, and $Tyr286_{Uganda}$ *vs.* $His286_{Brazil}$, as well as seven conservative changes (Supplementary Fig. 1). We also used the ZIKV NS1 structure to model complete DENV2 and WNV NS1 structures. The complete NS1 proteins have only minor differences in the electrostatic surface potentials of the dimer inner hydrophobic faces, as the protruding β-roll, "greasy finger" and aromatic expansion (115-123) are hydrophobic (Fig. 1d, Supplementary Fig. 3). In contrast, the surface potentials of the NS1 outer faces vary dramatically among flaviviruses. NS1 from both ZIKV strains display a negatively charged region on the outer face of the wing domain and the central portion of the β-ladder domain whereas DENV2 and WNV NS1 are positively charged or neutral in these regions (Supplementary Fig. 3). The sequence changes from $ZIKV_{Uganda}$ to $ZIKV_{Brazil}$ illustrate how genetic drift alters the appearance of the NS1 virulence factor as viewed by the innate immune system.

The structure of full-length ZIKV NS1 provides a solid molecular framework to begin understanding the multiple functions of this virulence protein. The structure of the wing flexible loop reveals an expanded surface for NS1 to associate with membranes during replication, to associate with immature virions during particle morphogenesis, and to facilitate the interactions necessary for the hexameric lipo-protein complex.

Online Methods

Construction, cloning and expression evaluation

The amino acid sequence for Zika strain MR766, the original 1947 Ugandan strain, was used to design a gene sequence codon-optimized for insect cell expression. A linear synthetic DNA was purchased from IDT. Cloning, production of baculovirus and small-scale expression evaluation were carried out as described previously[21].

Large-scale production and purification of NS1 protein

Infections at 1 L were carried out using *Sf*9 cells seeded at 2×10^6 cells/mL and infected with a multiplicity of infection (MOI) of two. Cells were harvested 72 hours after infection. The purification was carried out as previously described for WNV and DENV2 NS1 proteins[11].

Crystallization and structure determination

ZIKV NS1 crystals were grown at 4°C by vapor-diffusion equilibration of a 1:1 or 1:2 mixture of protein stock (~5 mg/mL NS1, 50 mM Tris pH 7.5, 50 mM NH_3SO_4, 10% glycerol) and reservoir solution (20% – 25% PEG 3350, 150 mM NH_3SO_4, 100 mM Tris pH 8.5). Crystals formed within one week, were harvested without additional cryoprotection, and flash-cooled in liquid nitrogen. Data were collected at GM/CA beamline 23-ID-D at the Advanced Photon Source at an X-ray energy of 12.0 keV (λ = 1.033 Å) using a Pilatus3 6M detector. A total of 360° of data were collected from a single crystal at 100 K using a 0.2° image width. Data were integrated and scaled using XDS[22] (table S1). The crystal structure was solved by molecular replacement from the WNV NS1 (PDB 4O6D[11]) as a search model using the program Phaser[23]. The asymmetric unit contains one dimer. Model building was carried out with Coot[24] and refinement with PHENIX[25]. Electrostatic surface potentials

were calculated with APBS[26]. The model was validated with MolProbity[27] and has excellent Ramachandran statistics (97% favored, 3% allowed, 0 outliers).

Negative-stain electron microscopy

Samples were prepared using the conventional negative staining protocol[28], and imaged at room temperature with a Tecnai T12 electron microscope (FEI Company) operated at 120 kV. 4122 particle projections were subjected to iterative stable alignment and classification with ISAC[29], producing 88 classes.

Supplementary Material

Refer to Web version on PubMed Central for supplementary material.

Acknowledgments

The work described in this report was supported by the Margaret J. Hunter Collegiate Professorship in the Life Sciences to J.L.S. and by the University of Michigan Life Sciences Institute. GM/CA@APS is supported by the NIH National Institute of General Medical Sciences (AGM-12006) and National Cancer Institute (ACB-12002). The Advanced Photon Source is a US Department of Energy (DOE) Office of Science User Facility operated by Argonne National Laboratory under Contract No. DE-AC02-06CH11357.

References

1. Gatherer D, Kohl A. Zika virus: a previously slow pandemic spreads rapidly through the Americas. J Gen Virol. 2016; 97:269–273. [PubMed: 26684466]
2. Dick GWA, Kitchen SF, Haddow AJ. Zika virus. I Isolations and serological specificity. Trans R Soc Trop Med Hyg. 1952; 46:509–520. [PubMed: 12995440]
3. Mlakar J, et al. Zika virus associated with microcephaly. N Engl J Med. 2016; 374:951–958. [PubMed: 26862926]
4. Calvet G, et al. Detection and sequencing of Zika virus from amniotic fluid of fetuses with microcephaly in Brazil: a case study. Lancet Infect Dis. 2016
5. Cao-Lormeau VM, et al. Guillain-Barré Syndrome outbreak associated with Zika virus infection in French Polynesia: a case-control study. Lancet. 2016; 387:1531–1539. [PubMed: 26948433]
6. Lazear HM, Diamond MS. Zika virus: New clinical syndromes and its emergence in the western hemisphere. J Virol. 2016; 90:4864–4875. [PubMed: 26962217]
7. Pierson, TC., Diamond, MS. Flaviviruses. In: Knipe, DM., Howley, P., editors. Fields Virology. Vol. 2. Wolters Kluwer; 2013. p. 747-794.
8. Muller DA, Young PR. The flavivirus NS1 protein: molecular and structural biology, immunology, role in pathogenesis and application as a diagnostic biomarker. Antiviral Res. 2013; 98:192–208. [PubMed: 23523765]
9. Watterson D, Modhiran N, Young PR. The many faces of the flavivirus NS1 protein offer a multitude of options for inhibitor design. Antiviral Res. 2016; 130:7–18. [PubMed: 26944216]
10. Gutsche I, et al. Secreted dengue virus nonstructural protein NS1 is an atypical barrel-shaped high-density lipoprotein. Proc Natl Acad Sci USA. 2011; 108:8003–8008. [PubMed: 21518917]
11. Akey DL, Brown WC, Dutta S, Konwerski J, Jose J, Jurkiw TJ, DelProposto J, Ogata CM, Skiniotis G, Kuhn RJ, Smith JL. Flavivirus NS1 structures reveal surfaces for associations with membranes and the immune system. Science. 2014; 343:881–885. [PubMed: 24505133]
12. Beatty PR, Puerta-Guardo H, Killingbeck SS, Glasner DR, Hopkins K, Harris E. Dengue virus NS1 triggers endothelial permeability and vascular leak that is prevented by NS1 vaccination. Science Transl Med. 2015; 7:304ra141.

13. Modhiran N, Watterson D, Muller DA, Panetta AK, Sester DP, Liu L, Hume DA, Stacey KJ, Young PR. Dengue virus NS1 protein activates cells via Toll-like receptor 4 and disrupts endothelial cell monolayer integrity. Science Transl Med. 2015; 7:304ra142.
14. Scaturro P, Cortese M, Chatel-Chaix L, Fischl W, Bartenschlager R. Dengue virus non-structural protein 1 modulates infectious particle production via interaction with the structural proteins. PLoS Pathog. 2015; 11:e1005277. [PubMed: 26562291]
15. Sirohi D, Chen Z, Sun L, Klose T, Pierson TC, Rossmann MG, Kuhn RJ. The 3.8 Å resolution cryo-EM structure of Zika virus. Science. 2016; 352:467–470. [PubMed: 27033547]
16. Kostyuchenko VA, Lim EX, Zhang S, Fibriansah G, Ng TS, Ooi JS, Shi J, Lok SM. Structure of the thermally stable Zika virus. Nature. 2016
17. Song H, Qi J, Haywood J, Shi Y, Gao GF. Zika virus NS1 structure reveals diversity of electrostatic surfaces among flaviviruses. Nat Struct Mol Biol. 2016; 23:456–458. [PubMed: 27088990]
18. Edeling MA, Diamond MS, Fremont DH. Structural basis of flavivirus NS1 assembly and antibody recognition. Proc Natl Acad Sci USA. 2014; 111:4285–4290. [PubMed: 24594604]
19. Youn S, Li T, McCune BT, Edeling MA, Fremont DH, Cristea IM, Diamond MS. Evidence for a genetic and physical interaction between nonstructural proteins NS1 and NS4B that modulates replication of West Nile virus. J Virol. 2012; 86:7360–7371. [PubMed: 22553322]
20. Muller DA, Landsberg MJ, Bletchly C, Rothnagel R, Waddington L, Hankamer B, Young PR. Structure of the dengue virus glycoprotein non-structural protein 1 by electron microscopy and single-particle analysis. J Gen Virol. 2012; 93:771–779. [PubMed: 22238236]
21. Brown WC, DelProposto J, Rubin JR, Lamiman K, Carless J, Smith JL. New ligation-independent cloning vectors compatible with a high-throughput platform for parallel construct expression evaluation using baculovirus-infected insect cells. Protein Expr Purif. 2011; 77:34–45. [PubMed: 21262364]
22. Kabsch W. XDS. Acta Crystallogr D Biol Crystallogr. 2010; 66:125–132. [PubMed: 20124692]
23. McCoy AJ, Grosse-Kunstleve RW, Adams PD, Winn MD, Storoni LC, Read RJ. Phaser crystallographic software. J Appl Crystallogr. 2007; 40:658–674. [PubMed: 19461840]
24. Emsley P, Cowtan K. Coot: model-building tools for molecular graphics. Acta Crystallogr D Biol Crystallogr. 2004; 60:2126–2132. [PubMed: 15572765]
25. Adams PD, Grosse-Kunstleve RW, Hung LW, Ioerger TR, McCoy AJ, Moriarty NW, Read RJ, Sacchettini JC, Sauter NK, Terwilliger TC. PHENIX: building new software for automated crystallographic structure determination. Acta Crystallogr D Biol Crystallogr. 2002; 58:1948–1954. [PubMed: 12393927]
26. Baker NA, Sept D, Joseph S, Holst MJ, McCammon JA. Electrostatics of nanosystems: application to microtubules and the ribosome. Proc Natl Acad Sci USA. 2001; 98:10037–10041. [PubMed: 11517324]
27. Davis IW, Leaver-Fay A, Chen VB, Block JN, Kapral GJ, Wang X, Murray LW, Arendall WB 3rd, Snoeyink J, Richardson JS, Richardson DC. MolProbity: all-atom contacts and structure validation for proteins and nucleic acids. Nucleic Acids Res. 2007; 35:W375–383. [PubMed: 17452350]
28. Ohi M, Li Y, Cheng Y, Walz T. Negative Staining and Image Classification - Powerful Tools in Modern Electron Microscopy. Biol Proced Online. 2004; 6:23–34. [PubMed: 15103397]
29. Yang Z, Fang J, Chittuluru J, Asturias FJ, Penczek PA. Iterative stable alignment and clustering of 2D transmission electron microscope images. Structure. 2012; 20:237–247. [PubMed: 22325773]

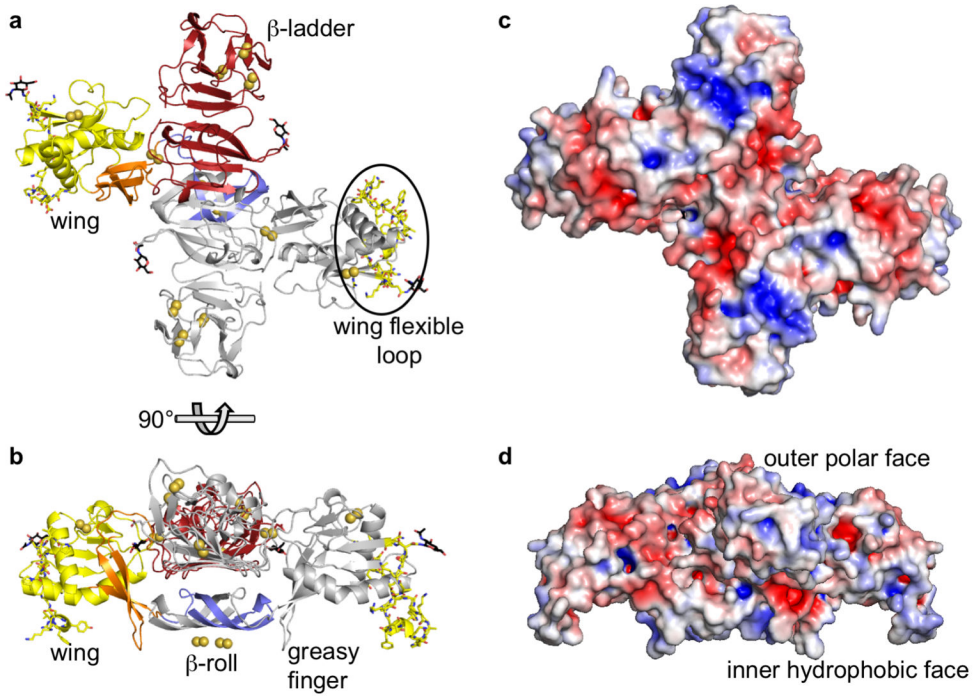

Figure 1. Zika virus NS1 dimer

(**a**) Ribbon representation of ZIKV NS1 dimer (Uganda strain MR-766) viewed from the outer face with one subunit in gray and the other subunit colored by domain: blue β-roll (amino acids 1-29); yellow wing domain (30-180) with orange connector subdomain and its "greasy finger" (159-163); red β-ladder domain (181-352). The wing flexible loop (yellow sticks on both subunits, circled in one subunit) includes amino acids 108-129 that were not observed in previous structures. Density was clear for all amino acids in one of two subunits in the crystal, and for all but residues 113-119 in the second. Glycosylation sites at Asn130 and Asn207 are indicated with black sticks, and disulfides with yellow double-spheres. (**b**) NS1 dimer viewed along β-ladder domain with the hydrophobic face pointed downward, rotated 90° about the horizontal axis relative to the view in (a). (**c**) Electrostatic surface representation of ZIKV NS1 dimer outer polar face, viewed as in (a). A symmetric dimer was created from the complete monomer. (**d**) Electrostatic representation viewed as in (b) with the inner hydrophobic face and aromatic protrusions pointed downward.

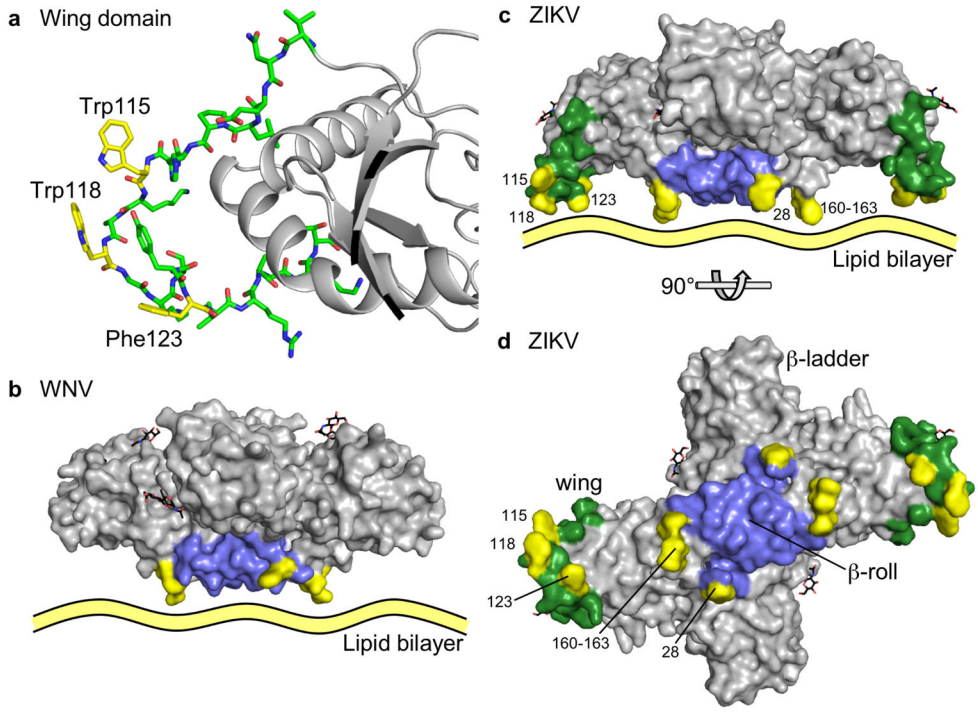

Figure 2. Wing flexible loop

(**a**) Ordered "wing tip" (residues 108-129) as green sticks with conserved Trp115, Trp118 and Phe123 in yellow. (**b**) Surface representation of WNV NS1 (end view, as in Fig. 1b). The structure lacks the wing flexible loop, which was disordered in the crystals. The β-roll (blue) and protruding aromatic "anchors" (amino acids 28 and 160-163 in yellow) define a limited hydrophobic surface. The β-ladder domain points towards the reader in the center of the image. (**c**) Surface representation of ZIKV NS1 showing the outward expansion of the hydrophobic surface with the wing flexible loop (green) and protruding aromatic anchors (amino acids 28, 115, 118, 123 and 160-163, yellow) in the same orientation and coloring as (b). (**d**) Surface representation of the hydrophobic face of the NS1 dimer, colored as in (b).

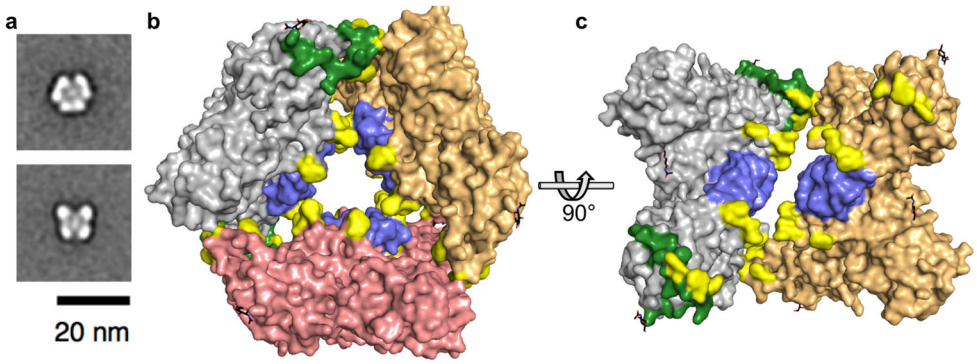

Figure 3. NS1 hexamer

(**a**) Representative EM class averages of ZIKV NS1 hexamers embedded in negative stain. (**b**) Top view of the ZIKV NS1 hexamer, modeled by superposition of three copies of the ZIKV NS1 dimer on dimers within the DENV2 NS1 hexamer. Individual dimers are colored gray, orange and salmon. In the gray NS1 dimer the wing flexible loop is green (amino acids 108-129); conserved, protruding aromatic side chains (28, 115, 118, 123, 160-163) are yellow; and the β-roll is blue. (**c**) Side view of the ZIKV NS1 hexamer model, colored as in (b) rotated 90° about the horizontal axis with the salmon-colored dimer removed to show how the aromatic side chains and hydrophobic β-roll line the interior of the hexamer.